Am J Physiol Gastrointest Liver Physiol 290: G250–G261, 2006.
First published July 7, 2005; doi:10.1152/ajpgi.00501.2004.

Intracellular Ca^{2+} and Zn^{2+} signals during monochloramine-induced oxidative stress in isolated rat colon crypts

Robert R. Cima,[1,2] J. Matthew Dubach,[1] Aaron M. Wieland,[1] Breda M. Walsh,[1] and David I. Soybel[1]

[1]*Department of Surgery, Brigham and Women's Hospital and Harvard Medical School, Boston, Massachusetts; and* [2]*Division of Colon and Rectal Surgery, Department of Surgery, Mayo Clinic, Rochester, Minnesota*

Submitted 8 November 2004; accepted in final form 25 May 2005

Cima, Robert R., J. Matthew Dubach, Aaron M. Wieland, Breda M. Walsh, and David I. Soybel. Intracellular Ca^{2+} and Zn^{2+} signals during monochloramine-induced oxidative stress in isolated rat colon crypts. *Am J Physiol Gastrointest Liver Physiol* 290: G250–G261, 2006. First published July 7, 2005; doi:10.1152/ajpgi.00501.2004.—During acute exacerbations of inflammatory bowel diseases, oxidants are generated through the interactions of bacteria in the lumen, activated granulocytes, and cells of the colon mucosa. In this study we explored the ability of one such class of oxidants, represented by monochloramine (NH_2Cl), to serve as agonists of Ca^{2+} and Zn^{2+} accumulation within the colonocyte. Individual colon crypts prepared from Sprague-Dawley rats were mounted in perfusion chambers after loading with fluorescent reporters fura 2-AM and fluozin 3-AM. These reporters were characterized, in situ, for responsiveness to Ca^{2+} and Zn^{2+} in the cytoplasm. Responses to different concentrations of NH_2Cl (50, 100, and 200 μM) were monitored. Subsequent studies were designed to identify the sources and mechanisms of NH_2Cl-induced increases in Ca^{2+} and Zn^{2+} in the cytoplasm. Exposure to NH_2Cl led to dose-dependent increases in intracellular Ca^{2+} concentration ($[Ca^{2+}]_i$) in the range of 200–400 nM above baseline levels. Further studies indicated that NH_2Cl-induced accumulation of Ca^{2+} in the cytoplasm is the result of release from intracellular stores and basolateral entry of extracellular Ca^{2+} through store-operated channels. In addition, exposure to NH_2Cl resulted in dose-dependent and sustained increases in intracellular Zn^{2+} concentration ($[Zn^{2+}]_i$) in the nanomolar range. These alterations were neutralized by dithiothreitol, which shields intracellular thiol groups from oxidation. We conclude that Ca^{2+}- and Zn^{2+}-handling proteins are susceptible to oxidation by chloramines, leading to sustained, but not necessarily toxic, increases in $[Ca^{2+}]_i$ and $[Zn^{2+}]_i$. Under certain conditions, NH_2Cl may act not as a toxin but as an agent that activates intracellular signaling pathways.

key words

INFLAMMATORY BOWEL DISEASES are thought to result from inappropriate activation of the mucosal immune system in response to normal flora (58, 60, 68). During acute exacerbations of these illnesses, reactive species are generated through the interactions of bacteria in the lumen, activated granulocytes, and cells of the colon mucosa. In inflamed human tissues and experimental models of colitis, oxidants and reductants derived from oxygen and nitrogen play a critical role in toxicity to microbes and injury to the "bystander" colon mucosa (2, 3, 39, 50, 58, 80). Presumed mechanisms of oxidant-induced injury of the epithelium include direct chemical attack on cell membranes and intracellular compartments, with consequences that include depolymerization of mucin; peroxidation of lipids; oxidation of structural proteins, enzymes, and carbohydrates; disorganization of DNA; and increased mucosal permeability. In addition, exposure to oxidants may activate intracellular signaling pathways that may exacerbate injury or, conversely, initiate protective responses in the inflamed mucosa. Affected pathways include protein kinase A and C activities, expression of heat-shock proteins, and modulation of NF-κB and effector pathways in apoptosis (24, 35, 52, 55, 58, 74). Of special interest is oxidant-induced release of the divalent cations, Ca^{2+} and Zn^{2+}, to the cytoplasm. When uncontrolled and in excess, such divalent cation signals can exacerbate tissue injury (10, 56, 67). When coordinated and in moderation, however, such signals may elicit secretory or protective responses that would prevent or arrest inflammation-induced injury (36, 69, 72).

In this study, we explored the ability of one class of oxidants, chloramines, to serve as agonists of Ca^{2+} and Zn^{2+} release to the cytoplasm of the colonocyte. The prototype in this class of oxidants, monochloramine (NH_2Cl), is produced through the reaction of neutrophil-derived hypochlorous acid (HOCl) with bacteria-derived ammonia (NH_3; see Refs. 25 and 63). NH_2Cl is relatively stable in aqueous environments and cell permeant (24, 25). Potential targets of NH_2Cl oxidation include molecules and structures in intracellular compartments as well as those on the cell membrane. Other chloramines species are generated by transfer of the oxidizing Cl· radical to amine groups of small organic acids such as taurine, lysine, or histamine (63). These chloramine species retain oxidant capacity but may not be able to permeate cell membranes. Molecular species capable of consuming or neutralizing the oxidant Cl· of chloramines include glutathione and other peptides and proteins (59) in which thiol (S-H) groups or clusters are integral to structure or enzymatic functions. Recent studies have implicated such thiol groups in structural proteins and enzymes that regulate intracellular homeostasis of divalent cations such as Ca^{2+} and Zn^{2+} (16, 46, 48, 77). These considerations led us to hypothesize that exposure to NH_2Cl may elicit a distinct profile of disturbances in intracellular divalent cation homeostasis in epithelial cells of the colon crypt.

METHODS

Solutions and reagents. Ringer solutions contained (in mM) 145 NaCl, 2.5 KH_2PO_4, 1.0 $MgSO_4$ or $MgCl_2$, 1 $CaCl_2$, 10 HEPES, and 10 glucose, pH = 7.4. Ca^{2+}-free Ringer contained all of the compounds in standard Ringer except Ca^{2+}, and, in addition, 500 μM EGTA was added. Intracellular buffer (ICB) contained (in mM) 125 KCl, 25 NaCl, 10 HEPES, 0.3 $CaCl_2$, 0.5 $MgCl_2$, 0.5 ATP, and 0.5 EGTA, pH = 7.25. Thapsigargin (THPS), ionomycin, and 1-hydroxypyridine-2-thione (pyrithione) were purchased from Sigma Chemical

Address for reprint requests and other correspondence: D. I. Soybel, Dept. of Surgery, Brigham and Women's Hospital, 75 Francis St., Boston, MA 02115 (e-mail: dsoybel@partners.org).

The costs of publication of this article were defrayed in part by the payment of page charges. The article must therefore be hereby marked "*advertisement*" in accordance with 18 U.S.C. Section 1734 solely to indicate this fact.

0193-1857/06 $8.00 Copyright © 2006 the American Physiological Society

Downloaded from ajpgi.physiology.org on January 26, 2008

and used from stock solutions containing DMSO. Carbachol (CCh; Sigma), dithiothreitol (DTT; Sigma), thimerosal (Sigma), *S*-nitroso-*N*-acetyl-D,L-penicillamine, (SNAP; Sigma), *N*,*N*,*N*′,*N*′-tetrakis(2-pyridyl-methyl) (TPEN; Molecular Probes), and 2-aminoethoxydiphenylborate (2-APB; Sigma) were dissolved in stock water and then brought up in Ringer (1:1,000) or dissolved directly in Ringer.

NH_2Cl was prepared as described previously (24, 62). Briefly, a 200-μl solution containing 500 mM NaOCl in water was added dropwise to 10 ml of 20 mM NH_4Cl and 5 mM Na_2HPO_4 in water at 0°C. This procedure resulted in a 5 mM NH_2Cl solution. Use of NH_2Cl was completed within 6 h of preparation, since we observed that it remained stable in Ringer solution at concentrations ranging from 50 to 200 μM with <10% loss of absorbance at 242 nm. TaurNHCl was generated under similar conditions by including taurine instead of NH_4Cl in the reaction mixture. Concentrations were verified by measuring absorbance in an ultraviolet spectrophotometer at 242, 292, and 252 nm for NH_2Cl, HOCl, and TaurNHCl, respectively. NH_2Cl concentration ([NH_2Cl]), HOCl concentration, and TaurNHCl concentration were then quantified using molar extinction coefficients reported previously (76). Solutions containing chloramines did not include and were not mixed with solutions containing DMSO to avoid direct consumption of oxidants that has been reported previously (65). We also performed in vitro studies indicating that DMSO can consume chloramines and, at high concentration (>1:100 vol/vol), interfere with measurements of Zn^{2+} in solution.

Crypt isolation. Anesthetic and procedures for killing used in these experiments were approved according to policies of Harvard Medical School. Male Sprague-Dawley rats (Charles River Laboratories) weighing ~300 g were anesthetized and underwent laparotomy. The distal colon was identified, and a 1- to 2-cm segment was removed. The viscus was opened and then rinsed in cold Ringer solution. As described previously (13), the colon was incubated in a Ca^{2+} chelation solution (966 mM NaCl, 1.5 mM KCl, 10 mM HEPES, 10 mM Tris, 27 mM NaEDTA or NaEGTA, 45 mM sorbitol, 28 mM sucrose, and 0.1% BSA) for 30 min at room temperature. After chelation, the tissue was manually shaken to liberate the crypts. The tissue was removed, and the solution was centrifuged at 200 rpm for 2 min. The supernatant was removed, and the pellet was resuspended in Ringer solution.

Dye loading: imaging and ratiometric measurements. Fura 2-AM and magfura 2-AM (Molecular Probes, Eugene, OR) were diluted in DMSO to a stock concentration of 1 mM. Suspended in 1.5 ml Eppendorf tubes, crypts were loaded in the dark at room temperature in Ringer solution with 8–10 μM fura 2-AM for 30 min. Subsequently, crypts were rinsed two times at 5-min intervals with Ringer solution, mounted on cover slips coated with poly-D-lysine, and transferred to the microscope stage (Nikon TE-2000). For studies utilizing fluozin 3, crypts were loaded under similar conditions for 20–30 min with 4–8 μM fluozin 3-AM. Coverslips were placed in a perfusion chamber for imaging studies, superfused with Ringer solution at room temperature.

Studies were performed using monochromator-based excitation (Applied Scientific Instrumentation, Eugene, OR). Emitted light was collected at 520 ± 15 nm. During studies with fura 2, fluorescence was monitored by alternating excitation at 340 and 380 nm. Data are presented as a ratio of cation-sensitive intensity at 340 nm over cation-insensitive intensity at 380 nm. For studies utilizing fluozin 3, crypts were excited at 488 nm. Digital images of crypts were captured using a digital CCD camera (Hammamatsu ORCA-ER). Images were processed using compatible software (Universal Imaging, Downington, PA) to yield background-corrected pseudocolor images. Images were acquired every 10 s to minimize photobleaching. Contributions of autofluorescence were measured and were negligible.

Data collection, analysis, and statistics. Simultaneous fluorescence measurements from a whole crypt were obtained, since signals from individual cells could not be discerned at this level of magnification. It has been reported previously that the cells of the crypt function as a unit and thus that signals in individual cells are reflected in regional measurements. Regions of interest selected for analysis included the base of the crypt (the region of cells closest to the submucosa) and the apex (the region closest to the lumen). Although responses were more robust in basal regions, no clear differences emerged between regions in responses to ionophores or to NH_2Cl. Thus results are reported for signals collected from the entire crypt.

Concentrations of extracellular Ca^{2+} in calibration solutions (containing TPEN and EGTA) were calculated using the internet-based program maxchelator (http://www.stanford.edu/%7Ecpatton/webmaxcS.htm). Dissociation constants (K_d) for fura 2 and fluozin 3 were calculated using the equation of Grynkiewicz et al. (26) formulated for both intensity-based and ratiometric dyes (http://www.molecularprobes.com/html). Data were summarized and reported as means ± SE. Comparisons were performed using ANOVA for multiple or sequential comparisons, as indicated.

RESULTS

Monitoring $[Ca^{2+}]_i$ in isolated colon crypts and controlling for interfering heavy metal divalent cations. Previous reports have demonstrated the feasibility of using dyes in the fura 2 and fluo 3 classes to monitor $[Ca^{2+}]_i$ levels in colon crypts in response to physiological stimuli (8, 40, 41). These approaches depend on assumptions (54) that have not been reported for primary cell preparations such as the colon crypt. Shown in Fig. 1, *A* and *B*, are digital images of a colon crypt loaded with fura 2-AM, recorded in visible light and during fluorescence

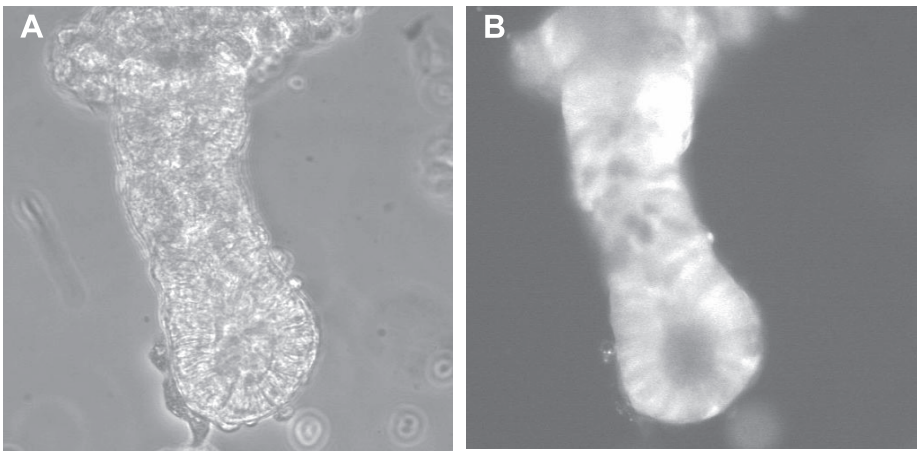

Fig. 1. Digital images in grayscale of an isolated rat colon crypt, loaded with fura 2-AM (8 μM) for 25 min. *A*: low visible light background. *B*: fluorescence excitation at 380 nm. Original magnification: ×30.

Downloaded from ajpgi.physiology.org on January 26, 2008

excitation at 380 nm. The first assumption is that the dye is localized almost completely within the cytpoplasm. Fluorescence intensity was monitored in crypts loaded with fura 2 at 340 and 380 nm, before and after exposure of crypts to 10 μM digitonin in ICB, an agent that permeabilizes the cell membrane without disturbing the integrity of organelles (31, 54). In five separate experiments, digitonin induced a marked decrease in fluorescence at both wavelengths, in all cases over 85%, indicating that fluorescence signals are the result of dye localized in the cytoplasm.

The second assumption of such fluorescence-based methods is that contributions of other interfering cations are negligible or can be controlled. All useful reporters respond to multiple divalent cations, although with different profiles of response (1, 26). In this regard, published reports suggest that, in cell-free systems, fura 2 increases fluorescence in response to Ca^{2+} (K_d ~145 nM), Zn^{2+} (K_d ~3 nM), and other metals not likely to interfere with fluorescence measurements, such as Cd^{2+} (K_d ~1 pM) and Co^{2+} (K_d ~9 nM; see Ref. 27). Responses to physiologically significant metals such as Cu^{2+} and Fe^{2+} are recognized but either cause quenching of signals or elicit responses opposite to those of Ca^{2+} and Zn^{2+} (1, 27, 38). However, release of such cations from intracellular pools or subcellular compartments could interfere with measurements of Ca^{2+} concentration ($[Ca^{2+}]$) when crypts are exposed to potentially toxic agents.

To evaluate such interference, we measured fura 2 signals during exposure of crypts to ionomycin, a cationophore able to translocate both Ca^{2+} and heavy metal divalent cations (15). In preliminary studies, crypts were exposed to 5 μM ionomycin in the presence of no added Ca^{2+} and 0.5 mM EGTA ($[Ca^{2+}]$ ~1 nM). Exposure to ionomycin rapidly increased the excitation ratio, indicating release of divalent cations to the cytoplasm. In six experiments, the interval and magnitude of recovery to baseline was highly variable. Such a response is characteristic of binding of the dye to a ligand of higher affinity, for example, Zn^{2+}. To evaluate this possibility, we monitored responses to ionomycin and varying $[Ca^{2+}]$ in the presence of TPEN, a known chelator for Zn^{2+} (K_d ~10^{-15} M) and other metal divalent cations (1). TPEN also exhibits a very low affinity for Ca^{2+} (K_d ~100 μM; see Refs. 1 and 21), thereby screening out contributions of interfering metal cations while permitting fura 2 to respond to cytoplasm Ca^{2+} signals in the physiological range (100 nM-1 μM; see Ref. 29). As shown in Fig. 2*A*, the presence of 20 μM TPEN permitted direct correlation of fura 2 signals to $[Ca^{2+}]_i$. We found the greatest responsiveness in the range of 100–400 μM, with diminished responsiveness both above and below this range. As shown in Fig. 2*B*, the responses within this range provide a method for in situ calibration that controls for contributions from interfering metal polyvalent cations. Inserting the data in the relationship of Grynkiewicz et al. (26), we calculate that, in situ in the colonic crypt, the K_d of fura 2 for Ca^{2+} is 282 ± 32 nM (average ± SE, n = 9). This value is somewhat higher than those reported previously in cultured cells but quite close to those reported for primary epithelial cell preparations such as the gastric gland (26, 27, 54). Using similar methods in studies of five isolated colon crypts, we determined that the in situ K_d of fura 2 for Zn^{2+} is 4.7 ± 0.6 nM (average ± SE), quite close to reported values (27). In these studies (n = 5 crypts), fura 2-loaded crypts were exposed to 40 μM pyrithione, a heavy metal specific ionophore, in 0 Ca^{2+} Ringer with varying concentrations of Zn^{2+} (0, 2.5, 5, 7.5, 10, and 1,000 nM). Experiments were also undertaken to ensure that pyrithione does not transport Ca^{2+} in the cytoplasm from either extracellular solution or from the cellular organelles (data not shown).

We next performed studies to evaluate whether the presence of TPEN might interfere with the ability of fura 2 to monitor physiological increases in $[Ca^{2+}]$. Crypts were perfused with Ringer solutions under control conditions and then during exposure to a combination of 100 μM CCh and 1 μM THPS, agents that cause Ca^{2+} release from intracellular stores and prevent reuptake, thereby maximizing accumulation in the cytoplasm (29–31). In addition, irreversible release of intracellular stores activates capacitative entry of Ca^{2+} from the extracellular spaces to the cytoplasm, resulting in irreversible accumulation of Ca^{2+} beyond physiological tolerable limits. As shown in Fig. 3, the presence of TPEN did not significantly alter $[Ca^{2+}]$ signals elicited by CCh/THPS or during capacitative entry. Together, these studies indicate that TPEN may be used to screen out contributions of other heavy metal cations while preserving the intracellular Ca^{2+} signals that are monitored by fura 2.

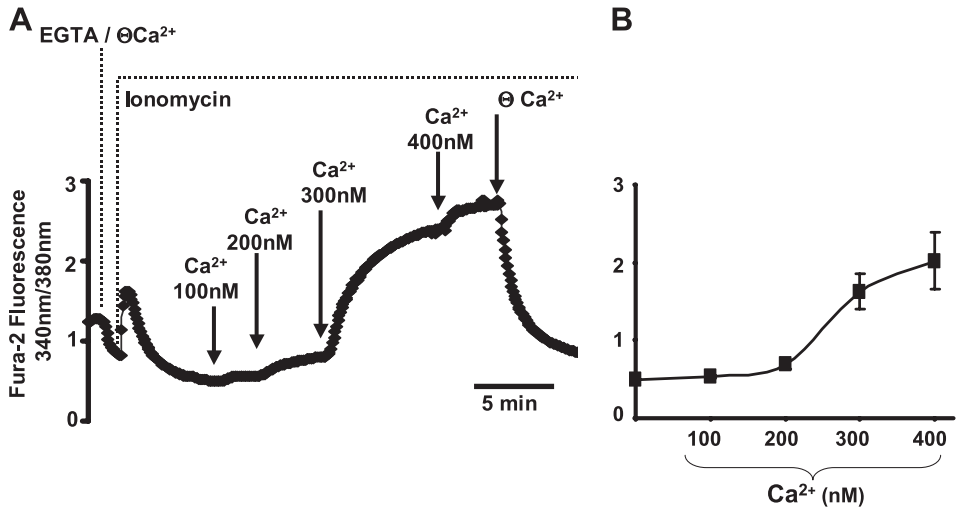

Fig. 2. Fura 2 signals in EGTA-isolated colon crypts during incremental increases in Ca^{2+} concentration ($[Ca^{2+}]$). Crypts were exposed to $[Ca^{2+}]$ varying from 100 to 400 nM in the presence of ionomycin (10 μM) and *N*,*N*,*N*′,*N*′-tetrakis(2-pyridyl-methyl) (TPEN, 20 μM). *A*: recording of fura 2 fluorescence in an individual crypt. ◆, Individual data points collected every 10 s. *B*: summary of calibration curves in 9 crypts using the same protocol as in *A*. Results are expressed as mean ± SE fluorescence excitation ratios (340/380 nm). With the use of averaged values in *B*, K_d of fura 2 for Ca^{2+} is 282 ± 32 nM.

Downloaded from ajpgi.physiology.org on January 26, 2008

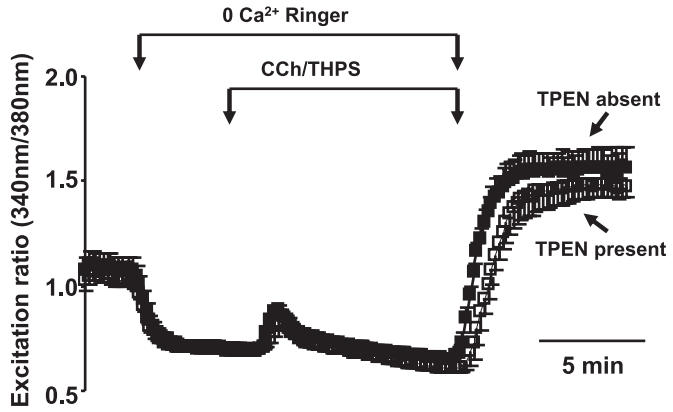

FIGURE 3

Fig. 3. Effect of TPEN on "pure" intracellular Ca^{2+} signals monitored by fura 2. Crypts were loaded with fura 2-AM and then exposed to Ringer solution containing 0 Ca^{2+} and 0.5 mM EGTA in the absence (■) or presence (□) of 20 μM TPEN. The presence of TPEN had no significant effect on signals generated during exposure to 100 μM carbachol (CCh) and 1 μM thapsigargin (THPS), which irreversibly empties intracellular stores. Also, TPEN had no significant effect on the magnitude of capacitative entry, monitored when extracellular Ca^{2+} was restored. Each line represents a mean of 5 individual experiments and expresses the mean ± SE of individual data points (10-s intervals) of the excitation ratio (340/380 nm).

Effects of NH_2Cl on $[Ca^{2+}]_i$ in isolated colon crypts. To evaluate the effects of NH_2Cl, we initially exposed isolated colon crypts to solutions containing [NH_2Cl] at 50, 100, and 200 μM. As summarized in Fig. 4, *A* and *B*, dose-dependent and largely irreversible increases were observed in the fluorescence excitation ratio. These basic observations led us to perform studies to determine the sources of these signals, including the contributions of *1*) extracellular Ca^{2+}, *2*) intracellular pools of non-Ca^{2+} heavy metal divalent cations, and *3*) physiologically regulated intracellular Ca^{2+} stores.

In the first set of studies, Ca^{2+} was removed from the perfusates, to which 0.5 mM EGTA was added to lower [Ca^{2+}] to ~1 nM. Crypts were exposed to different concentrations of NH_2Cl [0 (control), 50, 100, and 200 μM]. After a 5-min exposure, NH_2Cl was withdrawn. As shown in Fig. 5*A*, the excitation ratio decreased when Ca^{2+} was removed from the perfusate, confirming that extracellular Ca^{2+} plays an important role in preserving $[Ca^{2+}]_i$ under baseline conditions (17). During exposure to NH_2Cl, the signal increased dose dependently to a plateau but then partially reversed when NH_2Cl was withdrawn. The peak effects were greatly diminished compared with those observed in the presence of extracellular Ca^{2+} (Fig. 4), indicating that a significant component of the response to NH_2Cl is because of influx of extracellular Ca^{2+}.

In the second set of studies, we monitored fura 2 signals in crypts exposed to NH_2Cl in the presence of TPEN. Crypts were first exposed to 0 Ca^{2+} Ringer and 20 μM TPEN to eliminate contributions from extracellular Ca^{2+} and to chelate labile metal cations present in intracellular pools, respectively. Crypts were then exposed to 200 μM NH_2Cl for 5 min, allowed to recover in 0 Ca^{2+} Ringer, and then exposed to standard Ca^{2+}-Ringer. As shown in Fig. 6, preexposure of crypts to TPEN significantly reduced and delayed the peak

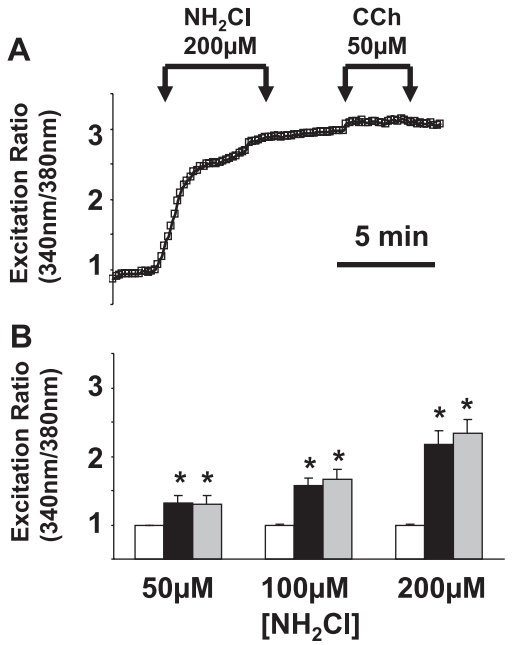

Fig. 4. Measurements of fura 2 signals during exposure of colon crypts to NH_2Cl. *A*: recording in an individual crypt exposed to 200 μM NH_2Cl. Recording begins with crypts perfused by standard Ringer solution, then exposure to NH_2Cl (5 min), and then standard Ringer. Note absence of reversibility. *B*: summary of responses to monochloramine at different doses (50, 100, and 200 μM). Data represent ratio before (open bars), during (black bars), and after (shaded bars) exposure to NH_2Cl. Results are expressed as means ± SE, with the *y*-axis indicating the excitation ratio (340/380 nm). *$P <$ 0.01 compared with baseline levels by ANOVA.

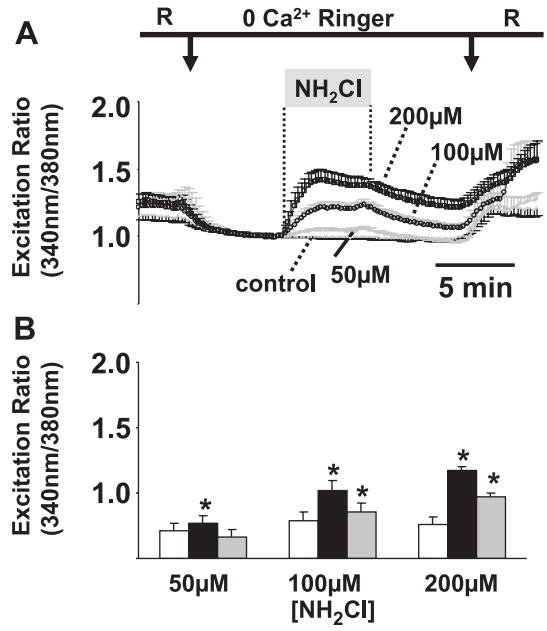

Fig. 5. Measurements of fura 2 signals during exposure of colon crypts to NH_2Cl, in the absence of extracellular Ca^{2+}. *A*: averaged responses to NH_2Cl at different doses [0 (control), 50, 100, and 200 μM). Each line represents responses in 5 or 6 separate experiments, each conducted in exactly the same sequence. Each experiment started with crypts perfused by standard Ringer, then exposure to 0 Ca^{2+}-Ringer (0.5 mM EGTA), exposure to NH_2Cl, removal of NH_2Cl, and then restoration of Ca^{2+}-Ringer. Each data point represents the mean ± SE of responses at each time point. *B*: key time points just before the peak response (open bars), during the peak response (black bars), and stablization after removal of NH_2Cl (shaded bars). Results are expressed as means ± SE, with the axis on *left* indicating the excitation ratio (340/380 nm). *$P <$ 0.01 compared with baseline levels by ANOVA. Arrows indicate where solutions change.

Downloaded from ajpgi.physiology.org on January 26, 2008

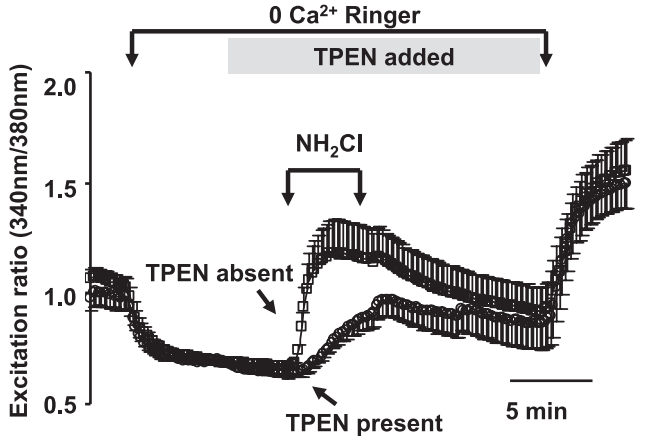

Fig. 6. Effects of TPEN on monochloramine-induced changes in fura 2 signals. □, Colon crypts exposed to 0 Ca^{2+} Ringer followed by addition of 200 μM NH_2Cl; ○, colon crypts exposed to 0 Ca^{2+} Ringer containing 20 μM TPEN, followed by addition of 200 μM NH_2Cl. Each data point represents the mean ± SE of 5 experiments. Slopes of the increase (after addition of NH_2Cl) are significantly different ($P < 0.01$ by linear regression). Note the exaggerated response to restoration of standard Ringer with physiological [Ca^{2+}] and lack of inhibition of extracellular calcium entry by TPEN.

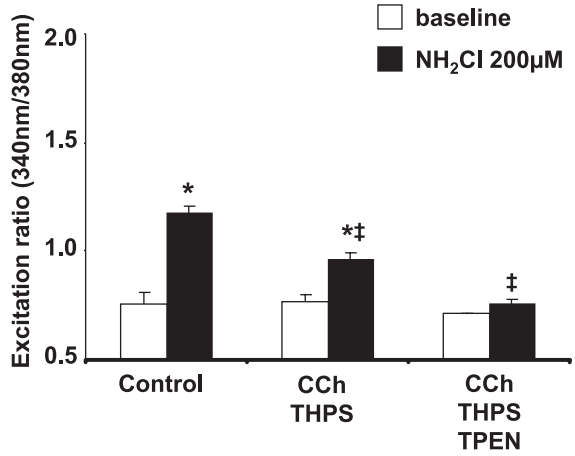

Fig. 8. Fura 2 signals were monitored during exposure to 200 μM NH_2Cl under baseline conditions (*left*), after 12 min irreversible depletion of intracellular stores by treatment with CCh (100 μM) and THPS (1 μM) (*middle*), and after depletion of stores and 5 min exposure to TPEN (20 μM) (*right*). *$P <$ 0.01 compared with pre-NH_2Cl baseline. ‡$P < 0.05$ vs. the response [change in (Δ) signal] to that observed under control conditions.

effect of NH_2Cl, indicating that a significant component of the NH_2Cl-induced signal is the result of heavy metal divalent cations. To further characterize the sensitivity to TPEN, crypts were exposed to NH_2Cl and then TPEN at the peak of the response. As shown in Fig. 7, exposure to TPEN at the peak response to NH_2Cl caused a significantly more rapid dissipation in the signal. These findings indicate that TPEN chelates labile metal divalent cations released by NH_2Cl and confirm that the fura 2 response is the result of release of both Ca^{2+} and non-Ca^{2+} metal divalent cations from within the cell.

We then performed studies to determine whether intracellular pools of Ca^{2+} released by NH_2Cl might include physiologically regulated intracellular stores. To deplete these stores, crypts were perfused in 0 Ca^{2+} Ringer solution alone or containing, in addition, 100 μM CCh and 1 μM THPS. Crypts were then exposed to 200 μM NH_2Cl. As shown in Fig. 8, there was a significant decrease in the response to NH_2Cl in crypts pretreated with CCh/THPS. These findings suggest that, in the absence of extracellular Ca^{2+}, release from intracellular stores is responsible for a component of the fura 2 signal achieved during exposure to NH_2Cl. In further studies, we first depleted the intracellular stores by exposing crypts to CCh/THPS and then monitored the response to NH_2Cl in the presence or absence of TPEN. As also shown in Fig. 8, the response to NH_2Cl was nearly abolished when TPEN was present. These findings indicate that, after elimination of extracellular Ca^{2+}, the fura 2 signal in response to NH_2Cl can be attributed largely to release from THPS-sensitive intracellular Ca^{2+} stores and intracellular pools of heavy metal cations that are sensitive to TPEN.

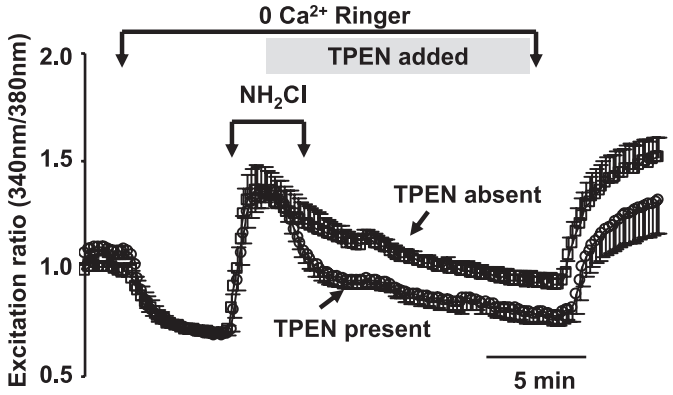

Fig. 7. Effects of TPEN on monochloramine-induced changes in fura 2 signals. □, Colon crypts exposed to 0 Ca^{2+} Ringer followed by addition of 200 μM NH_2Cl; ○, colon crypts exposed to 0 Ca^{2+} Ringer followed by addition of 200 μM NH_2Cl. At the peak of the NH_2Cl effect, crypts were then exposed to 20 μM TPEN. Slopes of the descent in the signal after NH_2Cl are significantly different ($P < 0.05$ by linear regression).

Studies were performed to more fully characterize NH_2Cl-induced disturbances in Ca^{2+} homeostasis, using 2-APB, a recognized inhibitor of store-operated channels. It has been reported that, under some experimental conditions, 2-APB may inhibit inositol trisphosphate receptor ($InsP_3$) actions, including release of intracellular stores. When such stores have been depleted, however, 2-APB has also been shown to block capacitative entry, independent of its effects on $InsP_3$ receptors (23, 43, 61). In these studies, fura 2-loaded crypts were exposed to NH_2Cl (200 μM) in Ca^{2+}-free Ringer containing TPEN (20 μM) to monitor an uncontaminated Ca^{2+} signal. After NH_2Cl-induced release of Ca^{2+} from intracellular stores, crypts were exposed to Ca^{2+}-Ringer (containing ~20 μM free TPEN) alone or, in addition, 100 μM 2-APB. A representative recording is shown in Fig. 9*A*, comparing responses of glands from the same harvest. In both recordings, peak effects and time course in response to NH_2Cl (in Ca^{2+}-free Ringer) and restoration of extracellular Ca^{2+} were similar to those observed previously in the presence of TPEN (Fig. 6). In the presence of 2-APB, added after store depletion by NH_2Cl, the increases in $[Ca^{2+}]_i$ in response to restoration of extracellular Ca^{2+} were reduced to levels expected in the absence of store-operated entry. These findings are summarized for the comparison in Fig. 9*B*, indicating that 2-APB-induced reductions in $[Ca^{2+}]_i$ were significant ($n = 7$ crypts in control and 2-APB groups).

Downloaded from ajpgi.physiology.org on January 26, 2008

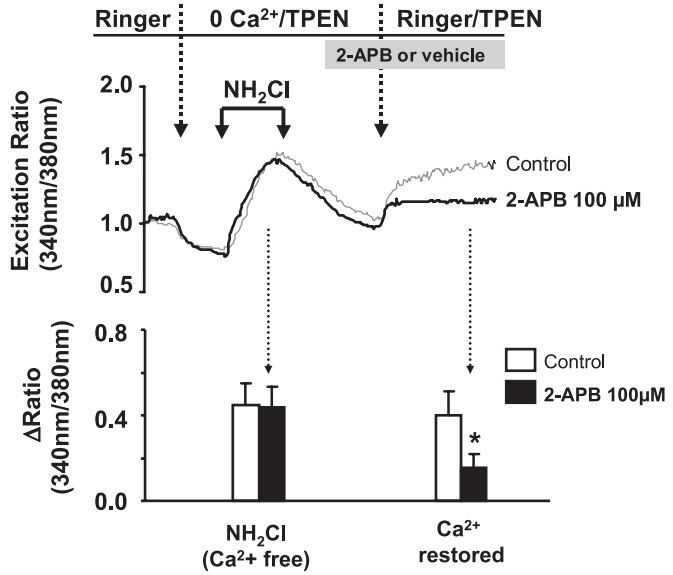

Fig. 9. Effects of 2-aminoethoxydiphenylborate (2-APB) on store-operated entry induced by NH_2Cl. *Top*: superimposed recordings from fura 2-loaded crypts from the same harvest. Both crypts were exposed to 200 μM NH_2Cl, in a protocol similar to that used in Fig. 6, with similar responses. As before, 20 μM TPEN was present to screen out contributions from heavy metal cations. *Bottom*: after removal of NH_2Cl, glands were exposed to 2-APB or vehicle (ethanol 1:1,000), and then extracellular Ca^{2+} was restored. In the presence of 2-APB, increases in intracellular $[Ca^{2+}]$ ($[Ca^{2+}]_i$; Δ ratio) were diminished significantly; $n = 7$ crypts in each group. $^*P < 0.05$.

Measurements of intracellular Zn^{2+} concentration in isolated colon crypts using fluozin 3. To more conclusively identify the TPEN-sensitive component of the divalent cation signal, we performed studies in isolated crypts loaded with a recently reported Zn^{2+}-sensitive fluorophore, fluozin 3 (27). This fluorophore has high affinity for Zn^{2+} (reported K_d ~10–20 nM) and little expected interference from physiological concentrations of Ca^{2+} (20, 64). Upon excitation, as shown in Fig. 10*A*, loading appears similar to that observed with fura 2. However, little has been determined about the characteristics of fluozin 3 loading. To verify that the majority of the dye was loading in the cytoplasm and not organelles, experiments similar to those performed on fura 2-loaded crypts were undertaken to monitor cytoplasmic loss of dye during exposure to digitonin. In four separate experiments, crypts were loaded with 5 μM fluozin 3 and 5 μM magfura 2 simultaneously (data not shown). Fluorescence signals were monitored from both reporters by exciting fluozin 3 at 488 nm and magfura 2 at 340/380 nm. In these studies, the simultaneous presence of Magfura 2 ensured permeabilization (36) and allowed us to compare the rates at which both reporters were lost during the permeabilization. Crypts were perfused with ICB containing 5 nM free Zn^{2+} and 40 μM pyrithione to increase the baseline signal intensity of fluozin 3. Digitonin (10 μM) was then added to induce the leakage of cytoplasmic dye. In each case, the intensity of fluozin 3 decreased by at least

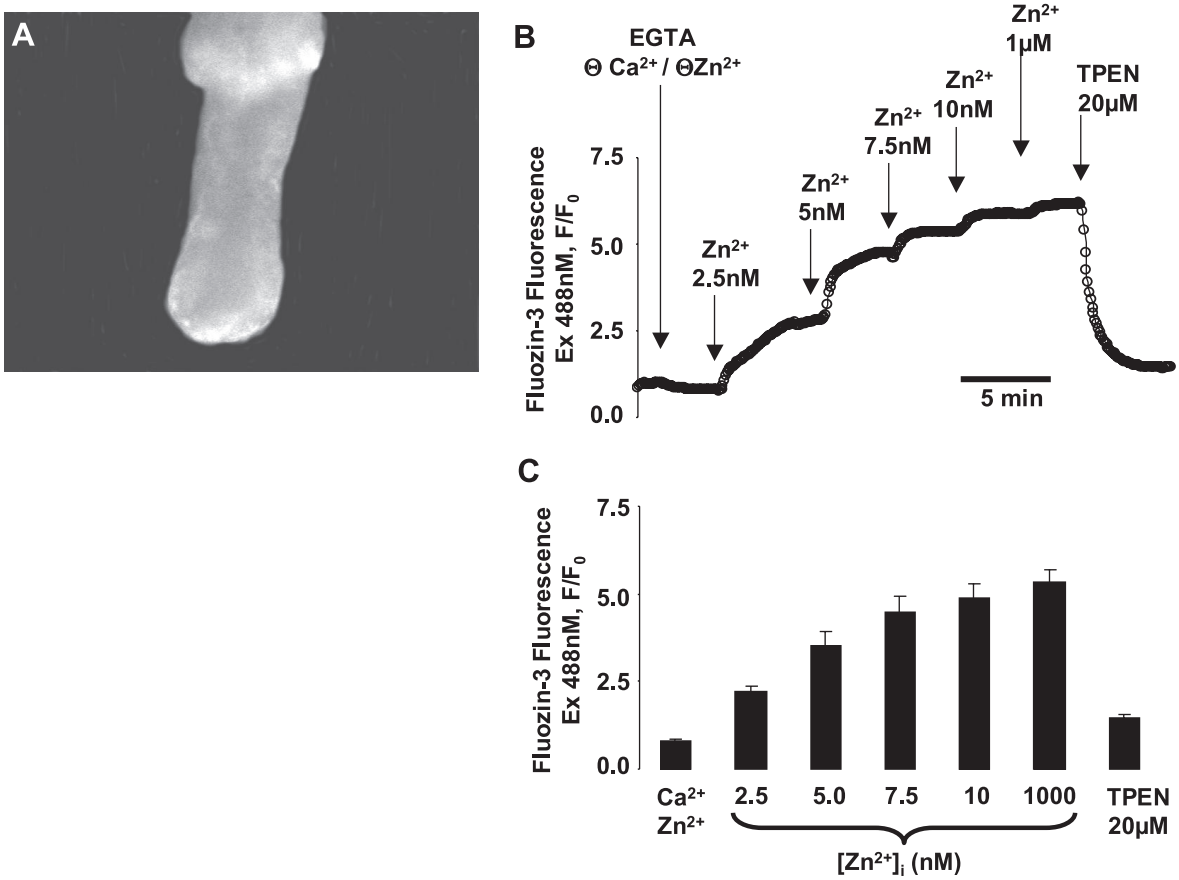

Fig. 10. *A*: digital images in grayscale of an isolated rat colon crypt loaded with fluozin 3-AM (4 μM) for 25 min. Fluorescence excitation was at 488 nm. *B*: recording of fluozin 3 fluorescence during exposure to different concentrations of Zn^{2+} buffered with EGTA in 0 Ca^{2+} Ringer with 40 μM sodium pyrithione. Fluorescence is expressed in arbitrary units of intensity normalized to starting values (F/F_o). *C*: summary of calibrations in 6 individual crypts. With the use of averaged values in *C*, K_d of fluozin 3 for Zn^{2+} is 4 ± 0.3 nM.

Downloaded from ajpgi.physiology.org on January 26, 2008

85% after addition of digitonin, and the decline rates of signals were not visibly different (data not shown).

In preliminary studies ($n = 4$), we observed that, when crypts were exposed to Ringer solutions containing ionomycin (10 μM), TPEN (20 μM), and [Ca^{2+}] (up to 1 μM), fluorescence signals were not altered, confirming that fluozin 3 signals are not influenced by increases in $[Ca^{2+}]_i$ within the physiological range. Responses were then monitored during exposure of fluozin 3-loaded crypts to varying concentrations of Zn^{2+} (0 nM, 2.5 nM, 5 nM, 7.5 nM, 10 nM, and 1 μM) in the presence of pyrithione (40 μM), a cationophore that is highly selective of non-Ca^{2+} metals such as Zn^{2+} and Fe^{2+} (75, 78). As shown in the recording in Fig. 10*B* and the summary of eight crypts in Fig. 10*C*, incremental increases in fluorescence were observed during increases in intracellular Zn^{2+} concentration ($[Zn^{2+}]_i$). Based on these studies, we calculate that in situ the K_d of fluozin 3 for Zn^{2+} is 4 ± 0.3 nM.

Effects of NH_2Cl on $[Zn^{2+}]_i$ in isolated colon crypts. To evaluate the effects of NH_2Cl, we exposed isolated colon crypts to solutions containing [NH_2Cl] of 50, 100, and 200 μM. As shown in Fig. 11*A*, rapid increases were observed in response to NH_2Cl, indicating that exposure to NH_2Cl causes a marked release of intracellular pools of Zn^{2+} within the colonocyte. The addition of pyrithione in a Zn^{2+}-free solution and in a 1-μM Zn^{2+} solution shows the ability of the ionophore to remove Zn^{2+} and the maximum signal capable under these experimental procedures, respectively. These signals were similarly quenched when TPEN was added to the perfusate ($n = 4$ experiments, data not shown), providing additional assurance

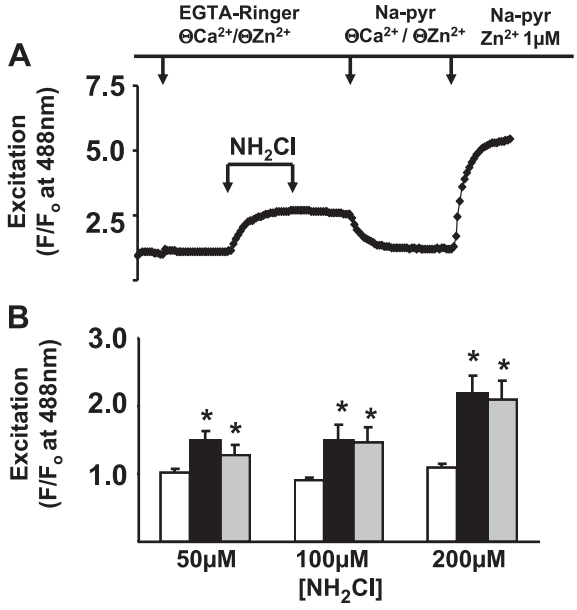

Fig. 11. Measurements of fluozin 3 signals during exposure of colon crypts to NH_2Cl. *A*: recording in an individual crypt exposed to 200 μM NH_2Cl in 0 Ca^{2+} Ringer. Recording begins with crypts perfused by standard Ringer solution, then removal of Ca^{2+}, followed by exposure to NH_2Cl (5 min), and recovery in 0 Ca^{2+} Ringer. Sodium pyrithione (Na-pyr, 40 μM) was added in the absence of Zn^{2+} followed by the addition of 1 μM Zn^{2+}. *B*: summary of responses to monochloramine at different doses (50, 100, and 200 μM). Results are expressed as means ± SE, with the *y*-axis indicating fluorescence intensity normalized to starting values (F/F_0). Data represent recordings before (open bars), during (black bars), and after (shaded bars) removal of NH_2Cl. *$P < 0.05$ compared with treatment before NH_2Cl.

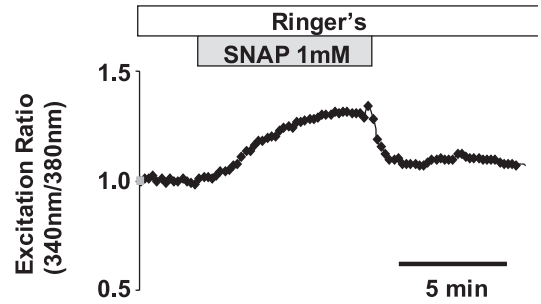

Fig. 12. Fura 2 fluorescence recording from an individual fura 2-loaded crypt exposed to the nitric oxide donor *S*-nitroso-*N*-acetylpenicillamine (SNAP).

that the signals were attributable to increases in $[Zn^{2+}]_i$. As shown in Fig. 11*B*, these effects were dose dependent. Based on calibration responses shown in Fig. 10*C*, it appears that labile $[Zn^{2+}]_i$ may increase to as much as 4–6 nM during exposure to 200 μM NH_2Cl.

Effects of NH_2Cl reactants, membrane-impermeable chloramines, and other control studies of reagents. In a series of control studies, we monitored fura 2 and fluozin 3 signals in isolated crypts during exposure to NH_3 (20 mM) and HOCl (200 μM), the reactants used to produce NH_2Cl. At these concentrations, no changes in signal were observed for either NH_3 ($n = 4$) or HOCl ($n = 4$), indicating that observed effects were the result of NH_2Cl and not its reactants (data not shown). Similarly, crypts were exposed to 200 μM taurine-NH_2Cl, a stable, but membrane-impermeant, chloramine species (24, 62). No alterations were observed in fura 2 or fluozin 3 signals (data not shown), indicating that the effects of NH_2Cl on $[Ca^{2+}]_i$ and $[Zn^{2+}]_i$ homeostasis are the result of its permeability in the cell membrane.

Additional control studies were performed to evaluate the possibility that NH_2Cl or its reactants might directly alter fluorescence properties of fura 2 or fluozin 3. In a cell-free chamber, each dye was placed in its free acid form, in the presence of EGTA-buffered solutions containing either 500 nM Ca^{2+} and 20 μM fura 2 or 2 nM Zn^{2+} and 20 μM fluozin 3. Addition of NH_2Cl, HOCl, or NH_3 all failed to alter baseline levels of fluorescence at the individual exciting wavelengths (340 and 380 nm for fura 2; 488 nm for fluozin 3). We also found no response to 100 μM peroxide, a precursor used by the neutrophil to generate HOCl. In addition, these reagents did not interfere with changes in fluorescence caused by doubling of divalent cation concentrations (data not shown).

We also performed studies to determine whether such effects might be observed in response to other recognized thiol oxidants, such as thimerosal (5, 45) and nitric oxide donors SNAP or 3-morpholinosydnonimine *N*-ethylcarbamide (SIN-1; see Refs. 18 and 19). In fura 2-loaded crypts ($n = 4$) exposed to thimerosal (100 μM), no responses were observed. In crypts exposed to the NO donor SNAP (1 mM), small but significant increases in fura 2 fluorescence were observed ($n = 5$ crypts, fura 2 excitation ratio 340/380 increasing from 1.00 ± 0.01 to 1.25 ± 0.05, $P < 0.005$; Fig. 12). Lower doses of SNAP (100 μM, $n = 5$) had no appreciable effect. These increases were not abolished in the presence of TPEN ($n = 3$ crypts). In addition, when fluozin 3-loaded crypts were exposed to SNAP (1 mM), little or no increase in fluorescence was observed. These findings indicate that SNAP-induced increases in the

Downloaded from ajpgi.physiology.org on January 26, 2008

fura 2 ratio are not attributable to accumulation of polyvalent cations such as Zn^{2+} and that Ca^{2+} is the accumulating ion. In other studies, the NO donor SIN-1 also elicited small but highly variable responses in fura 2-loaded crypts ($n = 4$). These observations indicate that release and accumulation of Ca^{2+} and Zn^{2+} are not observed uniformly in response to all thiol oxidants.

Intracellular thiols as targets of NH_2Cl oxidation. We performed studies to confirm that NH_2Cl-induced alterations in Ca^{2+} and Zn^{2+} homeostasis were because of release from thiol clusters that have been associated with proteins that bind or transport divalent cations (22, 42, 46, 48, 49, 59, 77). In one set of studies ($n = 4$), we pretreated crypts with DTT (1 mM), a known sulfhydryl reducing agent (47, 62), before exposure to 200 μM NH_2Cl. As shown in Fig. 13, as long as DTT was present in the perfusate, exposure to NH_2Cl did not elicit alterations in fura 2 signals. When DTT was removed, however, responses to NH_2Cl were immediately apparent. In other studies ($n = 4$), DTT reversed the effects of NH_2Cl when it was added after a peak effect was seen during NH_2Cl exposure. To determine whether the presence of DTT might alter the concentration of NH_2Cl in solution, we mixed 200 μM NH_2Cl and 1 mM DTT in a Ringer solution in a cell-free chamber. Measuring NH_2Cl absorbance at 242 nm, we found that the concentration of NH_2Cl did not decrease in the presence of DTT, indicating that the effects DTT were not attributable to consumption of NH_2Cl.

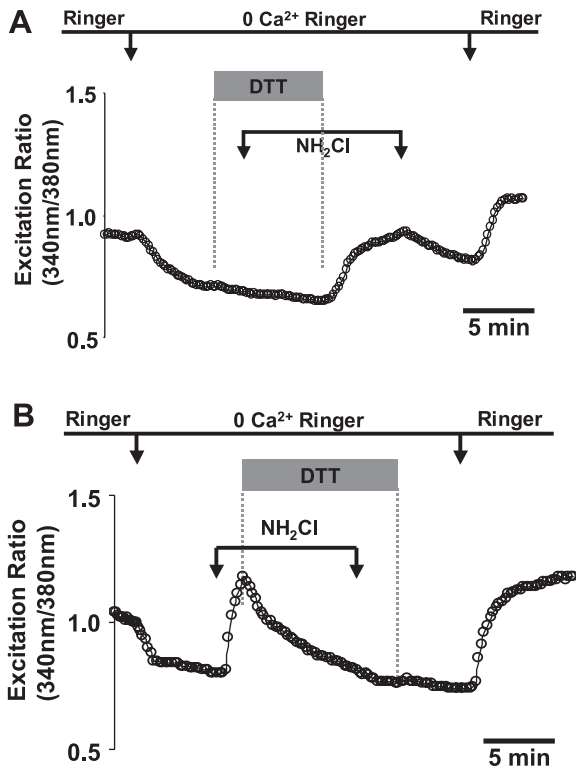

Fig. 13. Thiol reduction as a means of preventing or reversing NH_2Cl effects. *A*: recording in an individual crypt exposed to 200 μM NH_2Cl in 0 Ca^{2+} Ringer already containing 1 mM dithiothreitol (DTT). DTT was then removed with NH_2Cl remaining present. The crypt was allowed to recover in 0 Ca^{2+} Ringer, followed by addition of standard Ringer. *B*: recording in an individual crypt exposed to 1 mM DTT after initiation of responses to 200 μM NH_2Cl in 0 Ca^{2+} Ringer. NH_2Cl was later removed with DTT remaining present. Again, the crypt was allowed to recover in 0 Ca^{2+} Ringer, followed by addition of standard Ringer.

In an additional set of control studies, we monitored the ability of DTT to chelate Zn^{2+} or Ca^{2+}. Using fluozin 3 (K_d for Zn^{2+} ~3 nM) and fluozin 2 (K_d for Zn^{2+} ~1–2 μM; see Ref. 27), we monitored fluorescence (excitation 495 nm, emission 520 nm) of both reporters in cell-free KCl solutions (150 mM) containing standard total concentrations of Zn^{2+} using a 96-well plate fluorimeter. When fluozin 3 was present as the reporter, concentrations were calculated (maxchelator) to provide free Zn^{2+} concentration ($[Zn^{2+}]$) of 0.25 nM, 0.5 nM, 1.0 nM, 2.0 nM, 4.0 nM, 8.0 nM, and 16 nM if 500 μM EGTA (reported K_d for Zn^{2+} ~1.24 nM) was present as a chelator/buffer. In other experiments, when fluozin 2 was used as the reporter, concentrations were calculated (maxchelator) to provide free $[Zn^{2+}]$ of 0.25, 0.5, 1.0, 2.0, 4.0, 8.0, and 16 μM if 1 mM citrate (reported K_d for Zn^{2+} 17 μM) were present as a chelator/buffer. Standard curves using each reporter/chelator combination (fluozin 3/EGTA or fluozin 2/citrate) were generated, and fluorescence quenching of signals was compared when 1 mM DTT was used to replace the chelator for each reporter system. For two individual experiments, the relationship of Grinkiewicz et al. permitted us to calculate that the K_d of DTT for Zn^{2+} was 9.6 and 13.5 μM, well above any levels that might interfere with fluozin 3 measurements or that might account for the effects of DTT on $[Zn^{2+}]_i$ in the nanomolar range. In similar cell-free studies, the influence of DTT on Ca^{2+} content of solutions was negligible, indicating that observed effects of DTT on NH_2Cl-induced signals were not attributable to chelation of divalent cations.

DISCUSSION

To our knowledge, measurements of $[Zn^{2+}]_i$ have not been reported for epithelial cells of the colon mucosa. Moreover, previous reports utilizing fluorescence-based measurements of $[Ca^{2+}]_i$ in colonocytes have not taken into account contributions of other divalent cations, such as Zn^{2+}. To monitor isolated changes in $[Ca^{2+}]_i$ in the isolated colon crypt, we used a well-recognized, ratiometric fluorescent reporter, fura 2. In the presence of TPEN, which chelates non-Ca^{2+} metal divalent cations without interfering with levels of $[Ca^{2+}]_i$, fura 2 would monitor "pure" Ca^{2+} signaling responses to neurohumoral or pathological stimuli. To monitor changes in $[Zn^{2+}]_i$ directly, we used fluozin 3, a dye recently reported to be useful for measurements in the subnanomolar to nanomolar range.

Our studies indicate that NH_2Cl causes dose-dependent increases in $[Ca^{2+}]_i$ in native colon crypts of the rat. Further studies indicate that NH_2Cl-induced accumulation of Ca^{2+} in the cytoplasm is the result of release from intracellular stores, as well as store-operated entry from extracellular fluid. The duration of these increases is sustained beyond those associated with physiological stimuli (8, 41), but are partly reversible, even during exposure to NH_2Cl concentrations of up to 200 μM. We also noted that it was technically feasible to characterize these responses only when contributions of other divalent cations were screened out using the heavy metal chelator TPEN. In the presence of 20 μM TPEN, the increases in $[Ca^{2+}]_i$ are in the range of concentrations that are reported as physiological signals (11, 17, 41, 54). A comparison between responses to physiological agonists (Fig. 3) and to NH_2Cl (Fig.

Downloaded from ajpgi.physiology.org on January 26, 2008

6) indicates that, when contributions of other divalent cations are taken into account, the responses (perhaps 200–300 nM above baseline) lie within the range expected in response to neurohumoral stimuli.

We also found that exposure of crypts to NH_2Cl leads to dose-dependent increases in $[Zn^{2+}]_i$ in the range of 3–5 nM, which are sustained and not easily reversed. These effects on $[Ca^{2+}]_i$ and $[Zn^{2+}]_i$ are prevented by pretreatment with DTT, which shields intracellular thiol groups from oxidation by chlorinated oxidants. In addition, these effects are partially reversed by exposure to DTT, effects not attributable to chelation of Ca^{2+} or Zn^{2+}. These findings indicate that thiol groups in Ca^{2+}- and Zn^{2+}-handling proteins are susceptible to oxidation by chloramines, leading to sustained increases in $[Ca^{2+}]_i$ and $[Zn^{2+}]_i$. These findings offer the possibility that there is a range of concentrations over which NH_2Cl may not be toxic but instead stimulates release of physiological signals of oxidant stress in the colonocyte.

These studies raise three issues for discussion. The first issue is a technical one, namely, the strengths and limitations of fluorescence methods used to monitor intracellular divalent cation signals. Ca^{2+}-sensing fluorescent indicator dyes all are responsive to other polyvalent cations. Some potentially interfering ions (such as Cd^{2+}, Ba^{2+}, and La^{3+}) are excitatory (i.e., elicit responses similar to Ca^{2+}) but are not expected to interfere because they can only be added exogenously. In addition, some toxic cations (Mn^{2+}, Cd^{2+}, and Pb^{2+}) cause quenching or shifts in excitation spectra, rather than amplification of intensities; thus, they do not elicit responses similar to those of Ca^{2+}. Potentially interfering divalent cations include Fe^{2+}, Fe^{3+}, Cu^{2+}, and Zn^{2+}, which might be released from intracellular pools. The most widely used fluorescent reporter, fura 2, is quenched in response to Cu^{2+}, Fe^{2+}, and Fe^{3+}, but it responds to Zn^{2+} in a similar manner to Ca^{2+} (38). In fact, previous reports and manufacturer specifications indicate that, in vitro, fura 2 is more responsive to Zn^{2+} (K_d ~3–15 nM) than it is to Ca^{2+} (K_d ~150–300 nM; see Refs. 27, 38, and 54). Our calibration studies confirm these ranges of sensitivities to Ca^{2+} and Zn^{2+} in situ in cells of the rat colon crypt. These considerations suggest that, when fura 2 is used to monitor changes in $[Ca^{2+}]$, signals may include intracellular accumulation of Zn^{2+} in the nanomolar range.

Our studies demonstrate that fura 2 monitors increases in $[Zn^{2+}]_i$ under two sets of conditions. First, it appears that Zn^{2+} accumulates in the cytoplasm during exposure of the crypt to ionomycin, an ionophore frequently used to release Ca^{2+} from intracellular stores or to equilibrate Ca^{2+} in the cytoplasm with that in the extracellular fluid. Second, we observed release of Zn^{2+} during exposure to NH_2Cl, an oxidant that preferentially targets proteins containing thiolate clusters that bind or sequester heavy metal divalent cations. In both conditions, there are three considerations on which we base the conclusion that Zn^{2+} is the interfering ion. First, of the likely contaminating heavy metals, only Zn^{2+} elicits fluorescence responses similar to those of Ca^{2+}. Second, during exposure of crypts to ionomycin or NH_2Cl, fura 2 signals are reduced in the presence of TPEN, a chelator with profound affinity for Zn^{2+} (K_d ~10^{-15} M) and other heavy metals but not Ca^{2+} or Mg^{2+}. Third, exposure to ionomycin and NH_2Cl led to increases in fluorescence in crypts loaded with fluozin 3, a reporter with a high degree of preference for Zn^{2+} at nanomolar concentrations and virtual insensitivity to Ca^{2+} in the submicromolar range. Our studies do not necessarily exclude release of other divalent cations (for example Fe^{2+}, Fe^{3+}, or Cu^{2+}) during exposure to ionomycin or NH_2Cl. However, they would argue that the release of Zn^{2+}, which excites fura 2 fluorescence with high affinity, outweighs the effects of other metal polyvalent cations that would tend to quench fura 2 signals. Our findings also send a fundamental message that, in using fluorescent reporters to explore changes in $[Ca^{2+}]_i$ during exposure to oxidants, toxins, and relatively uncharacterized neurohumoral agonists, it is important to control or take into account accumulation of interfering polyvalent cations.

The second issue raised by these studies involves the mechanisms by which NH_2Cl causes accumulation of Ca^{2+} and Zn^{2+} within the cytoplasm of the colon crypt cell. With respect to $[Ca^{2+}]_i$, our studies indicate that NH_2Cl-induced accumulations are the result of release of Ca^{2+} from intracellular stores and influx from the extracellular microenvironment. When crypts were perfused with 0 Ca^{2+} Ringer and pretreated with CCh/THPS, exposure to NH_2Cl diminished the increases in $[Ca^{2+}]_i$, implying that THPS-sensitive stores are the major intracellular sources for the Ca^{2+} signal. These responses are attributable to thiol modification of Ca^{2+} transport processes, since DTT prevented and reversed effects of NH_2Cl on fura 2 signals.

The molecular basis for oxidant-induced release of Ca^{2+} from intracellular stores is not clear. In addition to direct modification of Ca^{2+} release channels in the membrane of the endoplasmic reticulum (16, 77), thiol oxidants might alter receptors regulating release of Ca^{2+} from stores to the cytoplasm. In this regard, both $InsP_3$ receptors (44) and ryanodine receptors (37) have been identified in colon crypts, the former having also been shown to support Ca^{2+}-dependent anion secretion (37). In other tissues, functional modification of either receptor has been demonstrated after exposure to thiol oxidants (14, 45), the latter in response to chloramines (14). These considerations suggest that NH_2Cl may find a broad spectrum of targets in the apparatus that regulates store emptying. Future studies, beyond the scope of the current report, may thus provide insight into the role that thiol redox state plays in regulating both store emptying and refilling.

Subsequent responses to solutions containing physiological levels of Ca^{2+}, however, make it clear that entry of extracellular Ca^{2+} is responsible for a major component of the NH_2Cl-induced signal (Figs. 6 and 7). Entry of extracellular Ca^{2+} might be because of influx through capacitative entry, activated when CCh- and THPS-sensitive stores are released (29–31). Alternatively, NH_2Cl-induced entry of extracellular Ca^{2+} might be independent of store emptying. In the present study, we found that 2-APB inhibits a significant component of NH_2Cl-stimulated entry of extracellular Ca^{2+}, arguing that NH_2Cl elicits its effects on extracellular influx through its effects on store depletion. It should be acknowledged, however, that, in the crypt configuration, it is difficult to directly evaluate the linkage between NH_2Cl-induced store emptying and influx of extracellular Ca^{2+}. It is possible that exposure to NH_2Cl may disengage store emptying and the "capacitative" entry that normally leads to store refilling. In cultured cell models, this separation of function (store release and store refilling) has been observed as a result of thiol modification through *S*-nitrosylation or alkylation (16, 42). Alternatively,

Downloaded from ajpgi.physiology.org on January 26, 2008

exposure to NH_2Cl might modify Ca^{2+} entry mechanisms that are independent of store emptying; in such cases, thiol modification has not been implicated (77). Further studies using reporters of intracellular stores may provide insight into these different possibilities (29–31). At the very least, our studies indicate that influx of extracellular Ca^{2+} supplies a major component of the sustained increase in $[Ca^{2+}]_i$ caused by NH_2Cl. It seems likely that the activation of such influx is at least partially independent of the effects of NH_2Cl on emptying of intracellular Ca^{2+} stores and is the result of thiol modification.

With respect to increases in $[Zn^{2+}]_i$, release of Zn^{2+} might be observed from specific Zn^{2+}-enriched subcellular compartments or from cytoplasm pools of Zn^{2+}-binding proteins that are susceptible to thiol modification. Subcellular compartments enriched in labile Zn^{2+} include acidic secretory compartments (20, 21) and under some conditions mitochondria (69). Cytoplasm pools of Zn^{2+}-binding proteins include metallothioneins, glutathione, heat shock proteins, and other peptides enriched in cysteine or methionine (32, 46, 48, 49). A number of studies have indicated that Zn^{2+} may be released by accumulation of oxidants that tend to attack thiol clusters in metallothioneins (32, 49). Currently, very little is reported on the mechanisms by which Zn^{2+} is transported in the colonocyte and distributed to intracellular pools and subcellular compartments. The current studies establish a reliable method for monitoring changes in intracellular $[Zn^{2+}]$ in colon crypts under physiological conditions and during oxidative stress. In addition, they provide evidence that NH_2Cl, and other oxidants that preferentially target S-H groups, may be highly effective in releasing Zn^{2+} to the cytoplasm of cells in the colon crypt.

The final issue raised by our studies involves the consequences of oxidant-induced increases in $[Ca^{2+}]_i$ and $[Zn^{2+}]_i$ in the colon crypt. We find that exposure to NH_2Cl elicits significant, but not necessarily unphysiological, increases in both $[Ca^{2+}]_i$ and $[Zn^{2+}]_i$.Our studies also suggest that chloramines may be considerably more powerful in eliciting these responses than are other recognized classes of thiol oxidants, most notably donors of nitric oxide. These observations raise intriguing questions regarding the structural specificity of different reactive nitrogen species, their targets, and potential intracellular pools buffering against their activity (thiol-rich molecules such as glutathione, metallothionein, etc). It is well recognized that increases in $[Ca^{2+}]_i$ trigger secretion in colon crypts (8, 51, 72, 73) and inhibit absorption in surface epithelium (28, 79), considered a "flushing" response that clears luminal bacteria and other noxious agents away from the mucosal surface (53, 57). In diverse in vitro cell culture models, agonist-stimulated increases in $[Ca^{2+}]_i$ enhance mitochondrial respiration and substrate utilization (34, 66). In excess, increases in $[Ca^{2+}]_i$ induce mitochondrial depolarization and the initiating events of apoptosis and/or cell necrosis (12, 56). In addition, studies in tissues outside the gastrointestinal tract have suggested that key metabolic and protective pathways are also sensitive to increases in $[Zn^{2+}]_i$. These pathways include enzymes of anaerobic glycolysis (4, 70) and the aerobic tricarboxylic acid cycle (10), specific isoforms of protein kinase C (6, 9, 71), downstream effects of cAMP signaling (36), modulation of mitochondrial respiration (69), and preexecution steps of apoptosis (7, 33). In the aggregate, these studies have suggested that uncontrolled accumulation of Ca^{2+} and Zn^{2+} may exacerbate mucosal injury. However, they also have offered the possibility that intracellular release of these divalent cations, coordinated and in moderation, may elicit responses that prevent, arrest, or possibly reverse inflammation-induced injury. The current set of observations provides a frame of reference for understanding the potential downstream effects of sustained increases in intracellular levels of $[Ca^{2+}]_i$ and $[Zn^{2+}]_i$, by providing quantitative estimates of the magnitude and time course of these increases.

In summary, we have adapted fluorometric approaches for monitoring changes in $[Ca^{2+}]_i$ and $[Zn^{2+}]_i$ in isolated crypts of the rat colon during exposure to oxidant stress. Our studies indicate that experimental approaches for monitoring $[Ca^{2+}]_i$ should control or take into account contributions from interfering polyvalent cations. When these factors are taken into account, it appears that NH_2Cl elicits increases in $[Ca^{2+}]_i$ that are sustained but certainly not much higher than those expected from normal signaling processes. These increases reflect contributions from emptying of physiologically regulated intracellular stores, as well as entry of extracellular Ca^{2+}, most likely through store-operated channels. In addition, increases in $[Zn^{2+}]_i$ are observed in response to NH_2Cl and probably reflect release from cytoplasm pools of metal-binding proteins such as metallothionein. Increases in $[Zn^{2+}]_i$ may thus act as signals of oxidative stress, potentially activating downstream responses that are protective and anti-apoptotic. Further studies will determine the role played by these signaling responses to unique thiol-directed oxidants such as NH_2Cl in injury and protection in acute colitis.

GRANTS

This study was supported by National Institute of Diabetes and Digestive and Kidney Diseases Grant R01 DK-44571 (to D. I. Soybel), by the Brigham Surgical Group Foundation (to D. I. Soybel), and by a Howard Hughes Medical Institute Student Fellowship (to A. M. Wieland).

REFERENCES

1. **Arslan P, Di Virgilio F, Beltrame M, Tsien RY, and Pozzan T.** Cytosolic Ca2+ homeostasis in Ehrlich and Yoshida carcinomas. A new, membrane-permeant chelator of heavy metals reveals that these ascites tumor cell lines have normal cytosolic free Ca^{2+}. *J Biol Chem* 260: 2719–2727, 1985.
2. **Babbs CF.** Oxygen radicals in ulcerative colitis. *Free Radic Biol Med* 13: 169–181, 1992.
3. **Blau S, Kohen R, Bass P, and Rubinstein A.** Relation between colonic inflammation severity and total low-molecular-weight antioxidant profiles in experimental colitis. *Dig Dis Sci* 45: 1180–1187, 2000.
4. **Brand IA and Kleineke J.** Intracellular zinc movement and its effect on the carbohydrate metabolism of isolated rat hepatocytes. *J Biol Chem* 271: 1941–1949, 1996.
5. **Bull R, Marengo JJ, Finkelstein JP, Behrens MI, and Alvarez O.** SH oxidation coordinates subunits of rat brain ryanodine receptor channels activated by calcium and ATP. *Am J Physiol Cell Physiol* 285: C119–C128, 2003.
6. **Cerda SR, Bissonnette M, Scaglione-Sewell B, Lyons MR, Khare S, Mustafi R, and Brasitus TA.** PKC-delta inhibits anchorage-dependent and -independent growth, enhances differentiation, and increases apoptosis in CaCo-2 cells. *Gastroenterology* 120: 1700–1712, 2001.
7. **Chai F, Truong-Tran AQ, Evdokiou A, Young GP, and Zalewski PD.** Intracellular zinc depletion induces caspase activation and $p21^{Waf1/Cip1}$ cleavage in human epithelial cell lines. *J Infect Dis* 182, *Suppl* 1: S85–S92, 2000.
8. **Cheng SX, Okuda M, Hall AE, Geibel JP, and Hebert SC.** Expression of calcium-sensing receptor in rat colonic epithelium: evidence for modulation of fluid secretion. *Am J Physiol Gastrointest Liver Physiol* 283: G240–G250, 2002.

Downloaded from ajpgi.physiology.org on January 26, 2008

9. **Chou SS, Clegg MS, Momma TY, Niles BJ, Duffy JY, Daston GP, and Keen CL.** Alterations in protein kinase C activity and processing during zinc deficiency-induced cell death. *Biochem J* 383: 63–71, 2004.
10. **Dineley KE, Votyakova TV, and Reynolds IJ.** Zinc inhibition of cellular energy production: implications for mitochondria and neurodegeneration. *J Neurochem* 85: 563–570, 2003.
11. **Duchen MR.** Mitochondria and Ca^{2+} in cell physiology and pathophysiology. *Cell Calcium* 28: 339–348, 2000.
12. **Duchen MR.** Mitochondria and calcium: from cell signalling to cell death. *J Physiol* 529: 57–68, 2000.
13. **Ecke D, Bleich M, Schwartz B, Fraser G, and Greger R.** The ion conductances of colonic crypts from dexamethasone-treated rats. *Pflügers Arch* 431: 419–426, 1996.
14. **Ehring GR, Kerschbaum HH, Fanger CM, Eder C, Rauer H, and Cahalan MD.** Vanadate induces calcium signaling, Ca2+ release-activated Ca2+ channel activation, and gene expression in T lymphocytes and RBL-2H3 mast cells via thiol oxidation. *J Immunol* 164: 679–687, 2000.
15. **Erdahl WL, Chapman CJ, Wang E, Taylor RW, and Pfeiffer DR.** Ionophore 4-BrA23187 transports Zn^{2+} and Mn^{2+} with high selectivity over Ca^{2+}. *Biochemistry* 35: 13817–13825, 1996.
16. **Favre CJ, Ufret-Vincenty CA, Stone MR, Ma HT, and Gill DL.** Ca^{2+} pool emptying stimulates Ca^{2+} entry activated by S-nitrosylation. *J Biol Chem* 273: 30855–30858, 1998.
17. **Frings M, Schultheiss G, and Diener M.** Electrogenic Ca2+ entry in the rat colonic epithelium. *Pflügers Arch* 439: 39–48, 1999.
18. **Fu Y, Porres JM, and Lei XG.** Comparative impacts of glutathione peroxidase-1 gene knockout on oxidative stress induced by reactive oxygen and nitrogen species in mouse hepatocytes. *Biochem J* 359: 687–695, 2001.
19. **Fujii T, Hamaoka R, Fujii J, and Taniguchi N.** Redox capacity of cells affects inactivation of glutathione reductase by nitrosative stress. *Arch Biochem Biophys* 378: 123–130, 2000.
20. **Gee KR, Zhou ZL, Qian WJ, and Kennedy R.** Detection and imaging of zinc secretion from pancreatic beta-cells using a new fluorescent zinc indicator. *J Am Chem Soc* 124: 776–778, 2002.
21. **Gerbino A, Hofer AM, McKay BM, Lau BW, and Soybel DI.** Divalent cations regulate acidity within the lumen and tubulovesicle compartment of gastric parietal cells. *Gastroenterology* 126: 182–195, 2004.
22. **Gow AJ, Chen Q, Hess DT, Day BJ, Ischiropoulos H, and Stamler JS.** Basal and stimulated protein S-nitrosylation in multiple cell types and tissues. *J Biol Chem* 277: 9637–9640, 2002.
23. **Gregory RB, Rychkov G, and Barritt GJ.** Evidence that 2-aminoethyl diphenylborate is a novel inhibitor of store-operated Ca2+ channels in liver cells, and acts through a mechanism which does not involve inositol trisphosphate receptors. *Biochem J* 354: 285–290, 2001.
24. **Grisham MB, Gaginella TS, von Ritter C, Tamai H, Be RM, and Granger DN.** Effects of neutrophil-derived oxidants on intestinal permeability, electrolyte transport, epithelial cell viability. *Inflammation* 14: 531–542, 1990.
25. **Grisham MB, Jefferson MM and Thomas EL.** Chlorination of endogenous amines by isolated neutrophils. *J Biol Chem* 259: 10404–10413, 1984.
26. **Grynkiewicz G, Poenie M, and Tsien RY.** A new generation of Ca^{2+} indicators with greatly improved fluorescence properties. *J Biol Chem* 260: 3440–3450, 1985.
27. **Haugland RP.** *Molecular Probes Product Information and Catalogue*. Eugene, OR: Molecular Probes, 1999.
28. **Hayashi H, Suzuki T, Yamamoto T, and Suzuki Y.** Cholinergic inhibition of electrogenic sodium absorption in the guinea pig distal colon. *Am J Physiol Gastrointest Liver Physiol* 284: G617–G628, 2003.
29. **Hofer AM, Fasolato C, and Pozzan T.** Capacitative Ca^{2+} entry is closely linked to the filling state of internal Ca^{2+} stores: a study using simultaneous measurements of ICRAC and intraluminal [Ca^{2+}]. *J Cell Biol* 140: 325–334, 1998.
30. **Hofer AM and Machen TE.** Direct measurement of free Ca in organelles of gastric epithelial cells. *Am J Physiol Gastrointest Liver Physiol* 267: G442–G451, 1994.
31. **Hofer AM and Machen TE.** Technique for in situ measurement of calcium in intracellular inositol 1,4,5-trisphosphate-sensitive stores using the fluorescent indicator mag-fura-2. *Proc Natl Acad Sci USA* 90: 2598–2602, 1993.
32. **Jacob C, Maret W, and Vallee BL.** Control of zinc transfer between thionein, metallothionein, and zinc proteins. *Proc Natl Acad Sci USA* 95: 3489–3494, 1998.
33. **Jiang D, Sullivan PG, Sensi SL, Steward O, and Weiss JH.** Zn^{2+} induces permeability transition pore opening and release of pro-apoptotic peptides from neuronal mitochondria. *J Biol Chem* 276: 47524–47529, 2001.
34. **Jouaville LS, Pinton P, Bastianutto C, Rutter GA, and Rizzuto R.** Regulation of mitochondrial ATP synthesis by calcium: evidence for a long-term metabolic priming. *Proc Natl Acad Sci USA* 96: 13807–13812, 1999.
35. **Karczewski JM, Peters JG, and Noordhoek J.** Prevention of oxidant-induced cell death in Caco-2 colon carcinoma cells after inhibition of poly(ADP-ribose) polymerase and Ca^{2+} chelation: involvement of a common mechanism. *Biochem Pharmacol* 57: 19–26, 1999.
36. **Klein C, Sunahara RK, Hudson TY, Heyduk T, and Howlett AC.** Zinc inhibition of cAMP signaling. *J Biol Chem* 277: 11859–11865, 2002.
37. **Kocks S, Schultheiss G, and Diener M.** Ryanodine receptors and the mediation of Ca^{2+}-dependent anion secretion across rat colon. *Pflügers Arch* 445: 390–397, 2002.
38. **Kress GJ, Dineley KE, and Reynolds IJ.** The relationship between intracellular free iron and cell injury in cultured neurons, astrocytes, and oligodendrocytes. *J Neurosci* 22: 5848–5855, 2002.
39. **Krieglstein CF, Cerwinka WH, Laroux FS, Salter JW, Russell JM, Schuermann G, Grisham MB, Ross CR, and Granger DN.** Regulation of murine intestinal inflammation by reactive metabolites of oxygen and nitrogen: divergent roles of superoxide and nitric oxide. *J Exp Med* 194: 1207–1218, 2001.
40. **Leipziger J, Kerstan D, Nitschke R, and Greger R.** ATP increases [Ca^{2+}]i and ion secretion via a basolateral P2Y-receptor in rat distal colonic mucosa. *Pflügers Arch* 434: 77–83, 1997.
41. **Lindqvist SM, Sharp P, Johnson IT, Satoh Y, and Williams MR.** Acetylcholine-induced calcium signaling along the rat colonic crypt axis. *Gastroenterology* 115: 1131–1143, 1998.
42. **Ma HT, Favre CJ, Patterson RL, Stone MR, and Gill DL.** Ca^{2+} entry activated by S-nitrosylation. *J Biol Chem* 274: 35318–35324, 1999.
43. **Ma HT, Venkatachalam K, Li HS, Montell C, Kurosaki T, Patterson RL, and Gill DL.** Assessment of the role of the inositol 1,4,5-trisphosphate receptor in the activation of transient receptor potential channels and store-operated Ca2+ entry channels. *J Biol Chem* 276: 18888–18896, 2001.
44. **Maranto AR.** Primary structure, ligand binding, and localization of the human type 3 inositol 1,4,5-trisphosphate receptor expressed in intestinal epithelium. *J Biol Chem* 269: 1222–1230, 1994.
45. **Marengo JJ, Hidalgo C, and Bull R.** Sulfhydryl oxidation modifies the calcium dependence of ryanodine-sensitive calcium channels of excitable cells. *Biophys J* 74: 1263–1277, 1998.
46. **Maret W.** Crosstalk of the group IIa and IIb metals calcium and zinc in cellular signaling. *Proc Natl Acad Sci USA* 98: 12325–12327, 2001.
47. **Maret W.** Oxidative metal release from metallothionein via zinc-thiol/disulfide interchange. *Proc Natl Acad Sci USA* 91: 237–241, 1994.
48. **Maret W.** Zinc and sulfur: a critical biological partnership. *Biochemistry* 43: 3301–3309, 2004.
49. **Maret W and Vallee BL.** Thiolate ligands in metallothionein confer redox activity on zinc clusters. *Proc Natl Acad Sci USA* 95: 3478–3482, 1998.
50. **McKenzie SJ, Baker MS, Buffinton GD, and Doe WF.** Evidence of oxidant-induced injury to epithelial cells during inflammatory bowel disease. *J Clin Invest* 98: 136–141, 1996.
51. **Merlin D, Jiang L, Strohmeier GR, Nusrat A, Alper SL, Lencer WI, and Madara JL.** Distinct Ca^{2+}- and cAMP-dependent anion conductances in the apical membrane of polarized T84 cells. *Am J Physiol Cell Physiol* 275: C484–C495, 1998.
52. **Musch MW, Sugi K, Straus D, and Chang EB.** Heat-shock protein 72 protects against oxidant-induced injury of barrier function of human colonic epithelial Caco2/bbe cells. *Gastroenterology* 117: 115–122, 1999.
53. **Nash S, Parkos C, Nusrat A, Delp C, and Madara JL.** In vitro model of intestinal crypt abscess: a novel neutrophil-derived secretagogue activity. *J Clin Invest* 87: 1474–1477, 1991.
54. **Negulescu PA and Machen TE.** Intracellular ion activities and membrane transport in parietal cells measured with fluorescent dyes. *Methods Enzymol* 192: 38–81, 1990.
55. **Ogino T, Kobuchi H, Sen CK, Roy S, Packer L, and Maguire JJ.** Monochloramine inhibits phorbol ester-inducible neutrophil respiratory burst activation and T cell interleukin-2 receptor expression by inhibiting inducible protein kinase C activity. *J Biol Chem* 272: 26247–26252, 1997.

Downloaded from ajpgi.physiology.org on January 26, 2008

56. **Orrenius S, Zhivotovsky B, and Nicotera P.** Regulation of cell death: the calcium-apoptosis link. *Nat Rev Mol Cell Biol* 4: 552–565, 2003.
57. **Parkos CA, Colgan SP, Delp C, Arnaout MA, and Madara JL.** Neutrophil migration across a cultured epithelial monolayer elicits a biphasic resistance response representing sequential effects on transcellular and paracellular pathways. *J Cell Biol* 117: 757–764, 1992.
58. **Pavlick KP, Laroux FS, Fuseler J, Wolf RE, Gray L, Hoffman J, and Grisham MB.** Role of reactive metabolites of oxygen and nitrogen in inflammatory bowel disease. *Free Radic Biol Med* 33: 311–322, 2002.
59. **Peskin AV and Winterbourn CC.** Kinetics of the reactions of hypochlorous acid and amino acid chloramines with thiols, methionine, and ascorbate. *Free Radic Biol Med* 30: 572–579, 2001.
60. **Podolsky DK.** Inflammatory bowel diseases. *N Engl J Med* 347: 417–429, 2002.
61. **Prakriya M and Lewis RS.** Potentiation and inhibition of Ca(2+) release-activated Ca(2+) channels by 2-aminoethyldiphenyl borate (2-APB) occurs independently of IP(3) receptors. *J Physiol* 536: 3–19, 2001.
62. **Prasad M, Matthews JB, He XD, and Akbarali HI.** Monochloramine directly modulates Ca^{2+}-activated K^+ channels in rabbit colonic muscularis mucosae. *Gastroenterology* 117: 906–917, 1999.
63. **Prutz WA.** Reactions of hypochlorous acid with biological substrates are activated catalytically by tertiary amines. *Arch Biochem Biophys* 357: 265–273, 1998.
64. **Qian WJ, Gee KR, and Kennedy RT.** Imaging of Zn^{2+} release from pancreatic beta-cells at the level of single exocytotic events. *Anal Chem* 75: 3136–3143, 2003.
65. **Quesada AR, Byrnes RW, Krezoski SO, and Petering DH.** Direct reaction of H_2O_2 with sulfhydryl groups in HL-60 cells: zinc-metallothionein and other sites. *Arch Biochem Biophys* 334: 241–250, 1996.
66. **Rizzuto R, Bernardi P, and Pozzan T.** Mitochondria as all-round players of the calcium game. *J Physiol* 529: 37–47, 2000.
67. **Rizzuto R, Pinton P, Ferrari D, Chami M, Szabadkai G, Magalhaes PJ, Di Virgilio F, and Pozzan T.** Calcium and apoptosis: facts and hypotheses. *Oncogene* 22: 8619–8627, 2003.
68. **Sartor RB.** Therapeutic manipulation of the enteric microflora in inflammatory bowel diseases: antiobiotics, probiotics and prebiotics. *Gastroenterology* 126: 1620–1633, 2004.
69. **Sensi SL, Ton-That D, Sullivan PG, Jonas EA, Gee KR, Kaczmarek LK, and Weiss JH.** Modulation of mitochondrial function by endogenous Zn2+ pools. *Proc Natl Acad Sci USA* 100: 6157–6162, 2003.
70. **Sheline CT, Behrens MM, and Choi DW.** Zinc-induced cortical neuronal death: contribution of energy failure attributable to loss of NAD(+) and inhibition of glycolysis. *J Neurosci* 20: 3139–3146, 2000.
71. **Stennicke HR and Salvesen GS.** Biochemical characteristics of caspases-3, -6, -7, and -8. *J Biol Chem* 272: 25719–25723, 1997.
72. **Sugi K, Musch MW, Di A, Nelson DJ, and Chang EB.** Oxidants potentiate Ca^{2+}- and cAMP-stimulated Cl^- secretion in intestinal epithelial T84 cells. *Gastroenterology* 120: 89–98, 2001.
73. **Tamai H, Gaginella TS, Kachur JF, Musch MW, and Chang EB.** Ca-mediated stimulation of Cl secretion by reactive oxygen metabolites in human colonic T84 cells. *J Clin Invest* 89: 301–307, 1992.
74. **Tamai H, Kachur JF, Baron DA, Grisham MB, and Gaginella TS.** Monochloramine, a neutrophil-derived oxidant, stimulates rat colonic secretion. *J Pharmacol Exp Ther* 257: 887–894, 1991.
75. **Tatsumi T and Fliss. H.** Hypochlorous acid and chloramines increase endothelial permeability: possible involvement of cellular zinc. *Am J Physiol Heart Circ Physiol* 267: H1597–H1607, 1994.
76. **Thomas EL, Grisham MB, and Jefferson MM.** Myeloperoxidase-dependent effect of amines on functions of isolated neutrophils. *J Clin Invest* 72: 441–454, 1983.
77. **van Rossum DB, Patterson RL, Ma HT, and Gill DL.** Ca^{2+} entry mediated by store depletion, S-nitrosylation, and TRP3 channels. Comparison of coupling and function. *J Biol Chem* 275: 28562–28568, 2000.
78. **Zalewski PD, Forbes IJ, and Betts WH.** Correlation of apoptosis with change in intracellular labile Zn(II) using zinquin [(2-methyl-8-p-toluenesulphonamido-6-quinolyloxy)acetic acid], a new specific fluorescent probe for Zn(II). *Biochem J* 296: 403–408, 1993.
79. **Zimmerman TW, Dobbins JW, and Binder HJ.** Role of calcium in the regulation of colonic secretion in the rat. *Am J Physiol Gastrointest Liver Physiol* 244: G552–G560, 1983.
80. **Zingarelli B, Szabo C, and Salzman AL.** Reduced oxidative and nitrosative damage in murine experimental colitis in the absence of inducible nitric oxide synthase. *Gut* 45: 199–209, 1999.

Downloaded from ajpgi.physiology.org on January 26, 2008